eCELLS & MATERIALS

OPEN ACCESS

IN VITRO EFFECTS OF PARTICULATE BONE SUBSTITUTE MATERIALS ON THE RESORPTION ACTIVITY OF HUMAN OSTEOCLASTS

G. Russmueller[1]*, L. Winkler[1], R. Lieber[2], R. Seemann[1], K. Pirklbauer[1], C. Perisanidis[1],B. Kapeller[2], E. Spassova[3], E. Halwax[4], W.P. Poeschl[1], K. Macfelda[2] and D. Moser[1]

[1]Department of Oral- and Maxillofacial Surgery, Medical University of Vienna, Austria.
[2]Department of Biomedical Research, Medical University of Vienna, Austria.
[3]AlgOss, Biotechnologies GmbH, Vienna, Austria.
[4]Institute of Chemical Technologies and Analytics, Technical University of Vienna, Austria.

Abstract

Much research has been done on bone cells, but only a few studies deal with biomaterial-induced effects on human osteoclasts, which may take on an important role in the successful regeneration of bone. In order to highlight such effects, human peripheral blood mononuclear cells (PBMCs) were extracted from venous blood, differentiated to osteoclasts and then cultured in, the presence of five particulate hydroxyapatite (HA)/β-tricalcium phosphate (TCP) biomaterials, on bovine bone slices and glass cover slips. The biomaterials, AlgOSS 50/50 (50 % HA/50 % TCP), AlgOSS 20/80 (20 % HA/80 % TCP), Algipore (98 % HA), Cerasorb (100 % TCP) and Bio-Oss (100 % HA) were chosen to assess their influence on cell morphology and numbers. Light microscopic evaluation was performed during ongoing cell culture. After 21 d of cultivation, the biomaterial-induced effects on osteoclastic resorption of the bone slices were evaluated by scanning electron microscopy (SEM). Osteoclast-like cells were identified by TRAP staining. All five biomaterials showed larger area fractions of resorbed bone than the control (5.6 ± 6.8 %), as measured on SEM images. The purely hydroxyapatite-based Algipore (9.8 ± 9.7 %) and Bio-Oss (7.9 ± 8.8 %) showed significantly elevated area fraction rates ($p \leq 0.05$) of bone resorption. Light Microscope evaluation revealed a significant, but inhibiting effect of Cerasorb ($p = 0.05$). These data indicated that introducing of small biomaterial hydroxyapatite particles may have improved the performance of bone substitute materials.

Keywords: Bone substitute materials, biomaterials, bone resorption, phagocytosis, human osteoclasts, *in vitro*, hydroxyapatite, tricalcium phosphate.

***Address for correspondence**: Guenter Russmueller, M.D., D.M.D., Medical University of Vienna, Department of Oral- and Maxillofacial Surgery, Währinger Gürtel 18-20, A-1090 Vienna, Austria.
Email: guenter.russmueller@meduniwien.ac.at

Introduction

In general, procedures for the regeneration of bone are aimed at stimulating and facilitating the growth of bone into defect sites and they should maintain the volume of regenerated bone. Autologous bone grafting is proven to be the most effective procedure for the regeneration of bone defects (Amini *et al.*, 2012). Since it has the highest osteoconductive, osteoinductive and osteogenetic potential, it represents the gold standard for bone grafting. However, donor site morbidity, limited amount of autologous bone, and graft resorption promoted interest in the use of bone substitute materials as an alternative to autologous bone, especially for the regeneration of smaller defects (Laurie *et al.*, 1984; Riachi *et al.*, 2014; Schaaf *et al.*, 2010). These bone substitute materials are categorized as being allogenous (bone harvested from same species), xenogenous (bone harvested from different species) or alloplastic (synthetic materials). They mainly offer osteoconductive properties and differ in their resorption kinetics (Kao and Scott, 2007; Taylor *et al.*, 2002).

To optimize clinical results, biomaterials featuring slower resorption kinetics can lead to higher volume stability, as complete biomaterial resorption does not seem to be a prerequesition for regeneration success (Jensen *et al.*, 2012; Schilling AF, 2006). To make up for the lack of osteoinduction by these materials, a combination of bone substitutes with autologous bone or bone marrow, has been found to be beneficial (Jensen *et al.*, 2006; Russmueller *et al.*, 2015).

Bone resorption is the physiological role of osteoclasts (Kylmaoja *et al.*, 2015; Teitelbaum, 2000). Despite this unique ability to resorb the organic and inorganic matrix of bone, osteoclasts share several characteristics with foreign body giant cells (ten

Harkel *et al.*, 2015; Wang *et al.*, 1997b). Both cell types are part of the mononuclear phagocyte system and are derived from hematopoietic stem cells, whereas osteoblasts originate from mesenchymal stem cells (Miyamoto and Suda, 2003). Osteoclast differentiation is induced by macrophage colony-stimulating factor (M-CSF) and the ligand of the receptor activator of nuclear factor kappa B (RANKL) (Vaananen and Laitala-Leinonen, 2008), a member of the tumor necrosis factor family (Yasuda *et al.*, 1998). M-CSF also stimulates progenitor cells to express RANKL. RANKL-activated osteoclast precursor cells fuse to form differentiated multinuclear osteoclasts (Schilling *et al.*, 2004).

The interaction between osteoclasts and bone substitute materials seems to be one central part of successful bone regeneration, and understanding of the process at the cellular level may be necessary to achieve valid modeling of biomaterial effects *in vivo* (Detsch and Boccaccini, 2015; van Blitterswijk *et al.*, 1985).

Osteoclastic bone resorption is coupled functionally with bone formation. Due to this intrinsic regulation, biomaterial-induced osteoclast function can influence bone formation (Kylmaoja *et al.*, 2015).

The microscopic structure and the particle size of bone substitute materials seem to have more of an impact on cell differentiation, and consequently on bone resorption and formation, than do chemical composition and solubility (Sabokbar *et al.*, 1998; Yamada *et al.*, 1997).

Currently, there are no standardized protocols for comparative testing of biomaterials and their effects on osteoclast function. Standardized testing of biomaterial degradation patterns is carried out at extreme pH levels (pH 3). However, promising degradation properties retrieved from such tests may emerge as less favorable when analyzed under *in vivo* conditions (Keller *et al.*, 2012; Zhang *et al.*, 2012). It therefore seems evident that *in vivo* degradation depends on more factors than merely on solubility. The influence of enzymes, proteins and cellular activity, especially osteoclasts, is crucial to biomaterial degradation (Yamada *et al.*, 1997). In an attempt to address these issues, several cell-based resorption assays are reported. They give useful information on how to develop and optimize bone substitute prior to clinical application (Friederichs *et al.*, 2015; Winkler *et al.*, 2010; Zhang *et al.*, 2012).

Sabokbar *et al.* (1998; 2003) and Wang *et al.* (1997b) describe the effects of small-sized particles on osteoclast function. Their findings suggested that particulate bone substitute materials enhance the activity of human osteoclasts cultivated from precursor cells *in vitro*. In order to assess such effects on bone resorption behavior and cell morphology, the PBMCs were not cultured directly on the respective biomaterials but on bovine bone slices or glass cover slips along with small-sized biomaterial particles.

Materials and Methods

Cell culture

All volunteers gave their written consent to participate in this study, and all procedures were conducted in accordance with the Declaration of Helsinki. After approval by the Institutional Review Board of the Ethics Committee of the Medical University of Vienna and Vienna General Hospital, EK 1092/2011, five healthy volunteers (three males, two females) were selected and venous whole blood (20 mL) was drawn from each individual by venipuncture and stored in EDTA tubes (GBO, Kremsmuenster, Austria) for further processing.

Mononuclear cells (PBMCs) were extracted from the peripheral blood of the five donors and these cells were differentiated to osteoclasts. Differentiation was carried out based on the original protocol of Flanagan and Massey (2003). Modifications were applied, according to Sabokbar and Athanasou (2003). The protocol was further modified after initial results were obtained, in order to improve repeatability and reproducibility (Table 1).

After dilution with phosphate buffered saline (PBS) (Sigma Life Science, St. Louis, MO, USA) in a 1:1 ratio, pipetting to 16 mL Ficoll-Paque PLUS (GE Life Science, Little Chalfont, UK) and centrifugation at 500 ×*g* without brake set off for 20 min, the layer of PBMCs was collected and mixed 1:1 with Dulbecco's Modified Eagle Medium (DMEM) (Sigma Life Science) and centrifuged at 350 ×*g* for 8 min. The

Table 1. Comparison of original and modified protocol used for osteoclast differentiation.

Procedure step	Original protocol (Flanagan and Massey, 2003)	Modified protocol
Ficoll-Paque centrifugation	350 ×*g* for 30 min. w/o brake set off	500 ×*g* for 20 min. w/o brake set off
Centrifugation after collection of cell layer	in 10 mL PBS with 350 ×*g* for 10 min	twice in 10 mL DMEM with 350 ×*g* for 8 min
Target cell count per well	2×10^5	5×10^5
Washing after incubation	washing with PBS+ antibiotics, then transfer to fresh well plates	no washing before transfer to new well plates
Additives to culture medium	30 ng/mL RANKL 25 ng/mL M-CSF	30 ng/mL RANKL 25 ng/mL M-CSF 100 nM dexamethasone 10 nM vitamin D_3

Table 2. Overview of analyzed bone substitute materials (Accorsi-Mendonca *et al.*, 2008; Dorozhkin, 2011; Ewers, 2005; Schopper *et al.*, 2003; Schopper *et al.*, 2005; Spassova, 2007; Tadic and Epple, 2004). The phase composition ratio was estimated from X-ray diffraction powder patterns (CuKα radiation) using the Rietveld method. ([a] No F− substitution in this phase.)

Biomaterial	Phase composition	Ratio [w/w]	Origin	Porosity & pore size	Commercial grain size
BM1 AlgOSS 50/50	**Calcium deficient ion substituted HA** $Ca_{5-x}Mg_x(PO_4)_{3-y}(CO_3)_y(OH_z,F_{1-z})$ **Mg-β-Tricalcium phosphate** $Ca_{18}Mg_2H_2(PO_4)_{14}$ **Calcite** $CaCO_3$	51.9 % 46.7 % 1.4 %	phycogenic; red marine algae	67 % 1-10 µm	2 sizes; 0.1-2.0 mm
BM2 AlgOSS 20/80	**Calcium deficient ion substituted HA** $Ca_{5-x}Mg_x(PO_4)_{3-y}(CO_3)_y(OH)^{[a]}$ **Mg-β-Tricalcium phosphate** $Ca_{18}Mg_2H_2(PO_4)_{14}$ **Calcite** $CaCO_3$	19.6 % 80.2 % 0.2 %	phycogenic; red marine algae	78 % 1-6 µm	2 sizes; 0.1-2.0 mm
BM3 Algipore	**Calcium deficient ion substituted HA** $Ca_{5-x}Mg_x(PO_4)_{3-y}(CO_3)_y(OH_z,F_{1-z})$ **Mg-β-Tricalcium phosphate** $Ca_{18}Mg_2H_2(PO_4)_{14}$ **Calcite** $CaCO_3$	97.8 % 1.9 % 0.3 %	phycogenic; red marine algae	78 % 1-10 µm	3 sizes; 0.3-2.0 mm

suspension was washed twice with 10 mL DMEM (Sigma Life Science) and the cell pellet resuspended with 3 mL of medium. For counting, by light microscopy, cells were stained with Trypan Blue (Sigma Life Science).

5×10^5 cells were placed in each well on bovine bone slices (diameter 6 mm, thickness 0.65 mm, IDS Immunodiagnostic Systems, Tyne & Wear, UK) and on glass cover slips (diameter 10 mm, Marienfeld-Superior, Lauda-Königshofen, Germany) and incubated at 37 °C, 5 % CO_2 and 95 % humidity for 3 h.

The bone slices and glass cover slips were then transferred into well plates containing DMEM medium, supplemented with 10 % fetal calf serum (FCS) (Gibco® by Life Technologies, Carlsbad, NM, USA), 100 U/mL penicillin and 100 µg/mL streptomycin (Gibco® by Life Technologies), 25 ng/mL M-CSF (R&D Systems, Minneapolis, MN, USA), 30 ng/mL RANKL (PeproTech, Inc., Rocky Hill, NJ, USA), 10 nM vitamin D_3 (Sigma Life Science) and 100 nM dexamethasone (Sigma Life Science).

After the cells attached onto the bone slices or the glass cover slips, they were transferred into new well plates. To allow sedimentation, the particulate biomaterials were added to the culture along with the supplemented DMEM medium. The respective bone substitutes were added with a target concentration of 100 µg/mL. To determine this target amount of biomaterial, a concentration series was run prior to cell culture experiments and measured by scanning electron microscopy (SEM). A concentration of 100 µg/mL gave an even biomaterial sedimentation, covering approximately half of the surface of the respective cover slips or bone slices.

The cells were cultivated for 21 d (at 37°C, 5 % CO_2 and 95 % humidity) and half the culture medium was changed every third day. Culture medium was removed by slow pipetting only from the outer edges of the wells, so as not to remove adherent cells or sedimented biomaterials at the bottom and center of the well, and new medium slowly added to the culture. Before this procedure, images of the glass cover slip containing wells were taken by light microscopy for evaluation of cell maturation.

After 21 d, the plates were fixed (2.5 % glutaraldehyde (Sigma Life Science), potassium-phosphate buffer 0.1 M (pH 7.4, Sigma Life Science)) and stored at 4 °C for at least 2 h and prepared for SEM. Five experimental groups and one control group were examined per donor. Groups BM1 to BM5 contained the five respective biomaterials; the control contained no bone substitute material.

Bone substitute materials

Biomaterials that were chemically based on high crystallinity forms of the two calcium orthophosphates, hydroxyapatite (HA) and β-tricalcium phosphate (β-TCP) or a combination of both were used (Table 2 and 3). Such compound materials, called biphasic bone substitute materials, are available in order to control the velocity of biodegradation by adapting the β-TCP to HA ratio (Chow, 2009; Schopper *et al.*, 2005; Sheikh *et al.*, 2015).

In general, HA ($Ca_{10}(PO_4)_6(OH)_2$) offers little chemical solubility (at 25 °C, −log (Ks) = 116.8) on a cellular basis with a slow biodegradation rate *in vivo* (Bauer, 2007; Chow, 2009). Solubility of HA changes when it is calcium deficient (at 25 °C, −log (Ks) ≈ 85) or ion substituted (F^-, at 25 °C, −log (Ks) = 120) (Dorozhkin, 2011). If such calcium phosphates feature high crystallinity, they show considerably lower solubility than so-called amorphous calcium phosphates (at 25 °C, −log (Ks) ≈ 25) (Dorozhkin, 2011).

Table 3. Characterization of particulate biomaterials. The d10, d50 and d90 values were assessed by SEM analysis. The crystallite sizes and crystallinity were estimated from X-ray diffraction powder patterns (CuKα radiation) using the Rietveld method.

	BM1 AlgOSS 50/50	**BM2** AlgOSS 20/80	**BM3** Algipore	**BM4** Cerasorb	**BM5** Bio-Oss
d_{10} [µm]	1.83	2.28	1.66	3.04	1.87
d_{50} [µm]	**3.73**	**4.72**	**3.97**	**6.68**	**4.08**
d_{90} [µm]	8.29	9.93	9.06	13.08	10.5
Crystallite size [nm]	44/99	49/38	60	420	19
Crystallinity [%]	70	81	77	100	83

In contrast, β-TCP is chemically more soluble (at 25 °C, −log (Ks) = 28.9) than HA and offers a higher biodegradation rate (Chow, 2009; Horch *et al.*, 2006). Similar to HA, ion substitution leads to changes in solubility of β-TCP (Mg^{2+}, at 25 °C, −log (Ks) ≈ 33) (Li *et al.*, 2009a). Despite the stoichiometric phase composition and β-TCP to HA ratio, bioreactivity can be influenced by crystallinity and crystallite size (Gallinetti *et al.*, 2014; LeGeros *et al.*, 2003).

BM1 (AlgOSS 50/50, AlgOss Biotechnologies, Austria), BM2 (AlgOSS 20/80, AlgOss Biotechnologies, Austria) and BM3 (Algipore, Dentsply Implants, USA) derive from two species of lime-incrusted naturally-grown red marine algae: *Corallina officinalis* and *Amphiroa ephedra*. These algae contain a highly porous three-dimensional hard tissue skeleton, consisting mainly of calcium carbonate bound as calcite ($CaCO_3$). This algal calcite is converted either into a monophasic calcium deficient ion substituted phycogenic HA (with traces of calcite an Mg-β-TCP), or into a biphasic biomaterial containing HA and Mg-β-TCP (with traces of calcite) by hydrothermal chemical transformation in alkaline aqueous phosphate solution (Table 2). By varying the addition of magnesium and tuning parameters of the hydrothermal process, the concentration ratio of HA and β-TCP can be controlled obtaining biphasic composites with a β-TCP content up to 95 % by weight (Spassova, 2007).

BM4 (Cerasorb, Curasan, Germany) is a fully synthetic substitute from pure phase β-TCP. It can be obtained by calcining of calcium-deficient hydroxypatite at temperatures over 800 °C and reflects the rhombohedral low temperature form of tricalcium phosphate (Destainville *et al.*, 2003).

BM5 (Bio-Oss, Geistlich Pharma, Switzerland) is a bone substitute originating from bovine material and consists of pure phase HA. The bovine material undergoes a low heat treatment (300 °C) and a chemical extraction process, by which organic components are removed but the natural structure of bone is maintained (Baldini *et al.*, 2011).

Because the commercially available grain sizes of the biomaterials did not match the requirements of our experiment, we ground specimens of each biomaterial (2.0 g) in a micronizing mill under aqueous conditions, washed them with ethanol and dried them at 110 °C. The samples were then sieved (mesh 40 µm) and sterilized by gamma radiation (25.5 kGy/min, exposure period of 26 h).

Phase abundances (weight percentages), crystallinity and crystallite sizes of the particulate biomaterials were estimated from X-ray diffraction powder patterns on a PANalytical X'Pert PRO powder diffractometer (Tables 2 and 3). Measurement conditions were CuK_α radiation (λ_1 = 0.154060 nm, λ_2 = 0.154441 nm), primary beam X-ray mirror (Bragg-Brentano, HD), X'Celerator detector, scan length 2.546°, recording time per scan length 25 s, scan range 2θ = 5-70°, total recording time approximately 11 min, rotation of samples during the measurement at 4 s/rotation. The measured X-ray diffraction patterns were analyzed using the Rietveld Method as implemented into the TOPAS program (version 4.1, Bruker AXS, Karlsruhe 2008). Chebyshev polynomes were used for the modeling of the background.

Structure data for the crystalline phases were taken from the Inorganic Crystal Structure Database (version 2016-2, FIZ Karlsruhe-Leopoldshafen): hydroxyapatite $Ca_{10}(PO_4)_6OH_2$, whitlockite $Ca_{18}Mg_2H_2(PO_4)_{14}$, ß-tricalcium phosphate ß-$Ca_3(PO_4)_2$, calcite $CaCO_3$, and corundum α-Al_2O_3. The latter phase (α-Al_2O_3) was required for the determination of crystallinity by adding a certain amount of the standard reference material (NIST 676a) to the original samples. The samples were measured under the conditions mentioned above, and their XRD patterns analyzed by using the TOPAS program. The amorphous phase abundance in a given sample can be calculated from the ratio of percentage corundum as determined to percentage corundum as known. This ratio must be > 1 for samples containing amorphous phase, and crystallinity (%) is 100 % − % amorphous phase. Crystallite sizes were estimated using the TOPAS program from the X-ray reflection widths (Scherrer equation, spherical crystallites, Fig. 4).

For assessment of particle size distribution (Table 3), the five particulate bone substitute materials were applied to glass cover slips and analyzed by SEM (JSM 6310, JEOL Ltd., Tokyo Japan). The mean Feret's Diameter of the particles was defined using a semi-automated image analysis system (NIS- Elements AR 2.3.0, Nikon Corporation).

Light microscopy

Before every change of culture medium, light microscope images of the respective glass cover slips were taken (IMT-2 microscope, Olympus, Tokyo, Japan) and stored on a local computer. In order to assess the quality of phenotypic cell morphology during ongoing cell culture, a score system was developed based on cell number and multinuclearity of cells per field of view (Barnaba *et al.*, 2012; Kurihara *et al.*, 1990) (Table 4). Scores ranged from Score 0 (PBMCs) to Score 3 (osteoclast-like morphology) (Fig. 1). Assessments were carried out by three individuals, working independently, and their results were averaged for statistical evaluation.

TRAP-staining

Tartrate-resistant acid phosphatase (TRAP) is an enzyme released by osteoclasts during bone resorption (Vaananen and Laitala-Leinonen, 2008). TRAP-staining provides standard cytochemical detection and quantification of osteoclasts (Kirstein *et al.*, 2006).

Table 4. Criteria for defining the phenotypic score for assessment by light microscopy.

Cell number per field of view	Multinucleated cells	Score
≥ 60	≥ 3	3
30-60	1-2	2
10-20	0-1	1
≤ 10	0	0

After 21 d of cultivation, the glass cover slips were treated with fixative solution (citrate, acetone, formaldehyde 37 %, Sigma Life Science) for 30 s and rinsed with double distilled water. A commercial acid phosphatase leucocyte kit (Sigma Life Science) was used for the TRAP-staining. Cells were treated with the staining solution (Fast Garnet GBC, sodium nitrite, H_2O_{dd}, Naphtol AS-BI phosphoric acid, acetate and tartrate solution) and incubated at 37 °C for 1 h. After rinsing, counterstaining with hematoxylin (Gill No 3) was carried out.

Two cover slips were analyzed per donor and group,. One was treated with tartrate solution,

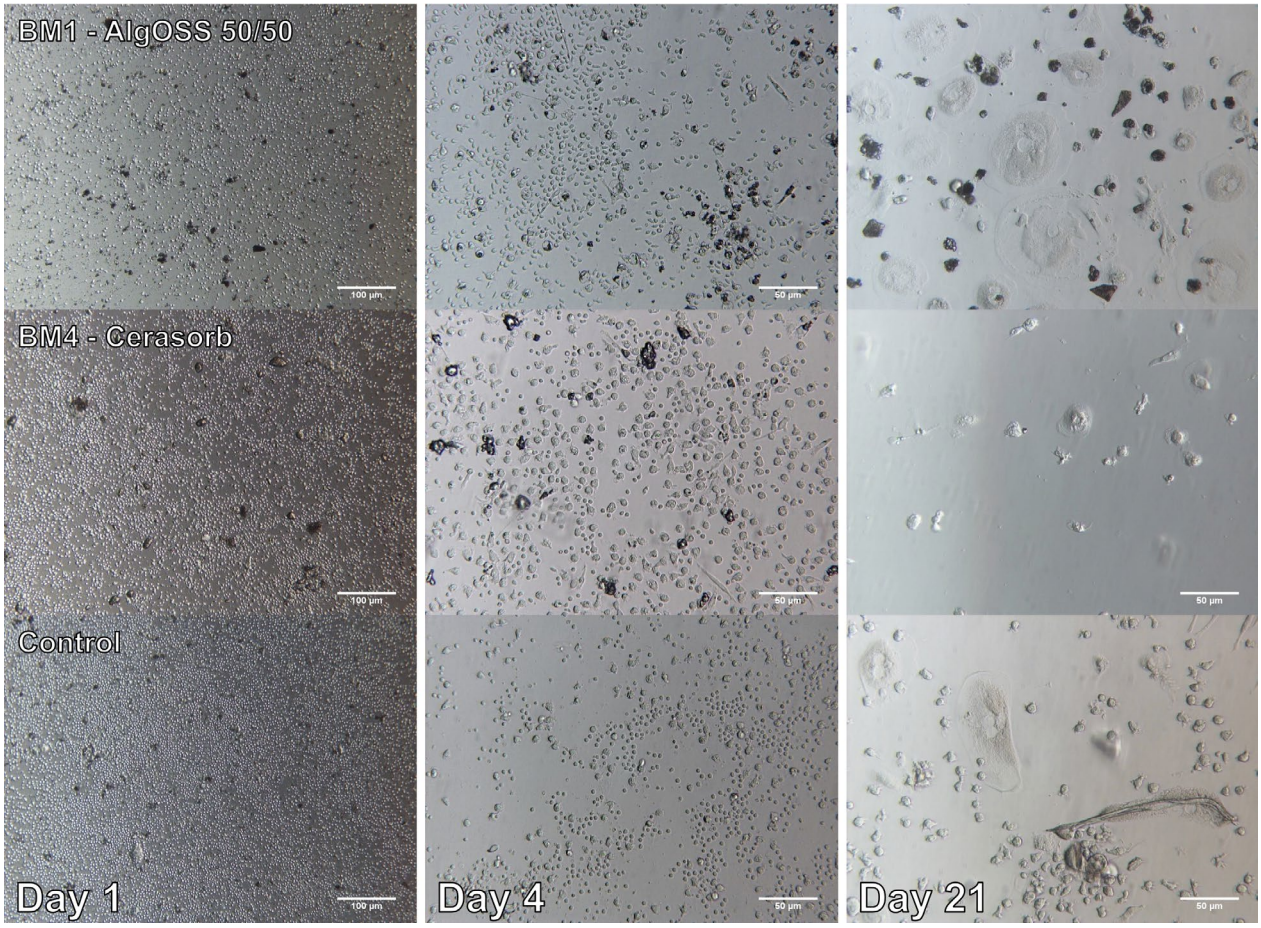

Fig 1. Cell differentiation. Representative images of PBMCs cultured and differentiated on glass cover slips toward osteoclast-like morphology. BM1-AlgOSS 50/50 (first line), BM4-Cerasorb (second line) and the control (third line) assessed on day 1 (first column), 4 (second column), and 21 (third column) of culture. All three groups feature no multinucleated cells on day 1 and therefore give a score of 0. On day 21, BM1 shows a high number of multinucleated cells (≥ 3) giving a score of 3. BM4 shows a low number of multinucleated cells (0-1) resulting in a score of 1 on day 21. Control shows a moderate number of multinucleated cells (1-2) giving a score of 2.

while the second served as negative control without specific staining. In order to quantify osteoclast-like cells, TRAP-positive cells were counted by light microscopy (BX60 microscope, Olympus, Tokyo, Japan). Reddish to brownish staining, featuring at least 3 nuclei, were classified as TRAP-positive (Kirstein *et al.*, 2006). For evaluation, TRAP-positive cells were summarized per group and donor.

SEM and histomorphometric analysis

4 bone slices and 2 glass cover slips were examined per donor and bone substitute, by SEM. In the control group without bone substitute, 2 bone slices were examined per donor. The bone slices containing cells and their respective biomaterial particles were dehydrated in a graded ethanol series, and critical point dried (Polaron CPD7501, Quorum Technologies, East Sussex, UK). For detection of the resorption lacunae, a confluent cell layer was removed prior to imaging by 'dabbing' with an adhesive strip. The samples were fixed on specimen mounts, coated with gold (Polaron SC7620 sputter coater, Quorum Technologies) and analyzed by SEM (JSM 6310 scanning electron microscope, JEOL, Tokyo, Japan) using an accelerating voltage of 15 kV. For histomorphometry, digital SEM images (15× magnification) of every bone slice and glass cover slip were taken.

To quantify osteoclastic resorption activity, the SEM images underwent histomorphometric analysis (ImageJ, National Institutes of Health, Bethesda, ML, USA). A "region of interest" (ROI) was standardized for every slice. The ROI included the maximum area of the bone slices excluding the very margin of the slices. The bottom arc was skipped because of the presence of automated annotations by the SEM. The photographs were inverted, brightness adapted, and the background was removed to diminish the consistent gray level. A threshold for gray levels was determined and area fractions of osteoclastic resorption pits were assessed (2**d**,**e**).

Statistics

Collected data were converted into descriptive statistics and their statistical significance assessed using a generalized linear model (GLM). As Poisson distribution is considered to be the best method for modeling areas, this distribution was used in the GLM to model the area fraction of resorbed bone on the respective bone slices. The cell-maturing score, TRAP-positive cells, and area fractions of resorbed bone were estimated by the biomaterial (BM) as dummy factors, the control group served as a baseline (intercept). Each effect was tested using Wald's Test, and a p-value of < 0.05 was defined as being significant. A *post-hoc* power analysis was performed in support of a sample size of five independent experiments (blood donors). To evaluate the inter-rater reliability (IRR) of the scoring system in light microscopy, a Fleiss' Kappa for more than two raters was calculated. All calculations were performed using the statistical programming environment "R" (version 2.15.1, Vienna, Austria).

Results

Light microscopy

To determine the influence of the particulate biomaterials on the phenotypic differentiation of PBMCs towards osteoclast-like morphology on the days that the culture medium was changed, cells cultured on glass cover slips were evaluated by light microscopy. On day 1 of culture, in all groups, only PBMCs (score 0) were found. Despite insignificant differences in maturing on day 4, all biomaterial groups, including the control, were at a similar stage of osteoclast-like morphology (score 1.79 ± 0.06) on day 7. After day 7, cell morphology differed greatly between the tested groups, but remained fairly stable from day 11 to day 21 in all groups. BM1 (AlgOSS 50/50) reached the highest overall levels of osteoclast-like morphology and cell number (score 2.45 ± 0.91), contrary to BM4 (Cerasorb), which showed a statistically significant inhibition ($p = 0.004$) throughout the observational period (score 1.27 ± 0.51). The other groups (BM2, BM3, BM5, and control) had comparable scores from day 11 onwards, with a slight increase towards the end. In addition, statistical evaluation featured a significant effect of the factor "day" ($p = 0.049$), indicating more pronounced osteoclastic cell morphology and cell number with the progress of time (Fig. 5, Table 5). Estimation of inter-rater reliability (IRR) for the semi-quantitative evaluation by light microscopy showed a Fleiss' Kappa of 0.495 for three observers (H_0(kappa = 0), H_1(kappa > 0): $p < 0.001$), indicating moderate agreement.

TRAP-staining

For the cytochemical detection of osteoclastic differentiation, PBMCs were cultured on glass cover slips and TRAP stained after 21 d of culture. Despite clear indications by light microscopy of osteoclast-like cell morphology, only few cells reached standard positive TRAP staining criteria (cells with reddish to brownish staining with ≥ 3 nuclei). Surprisingly, most TRAP-stained cells had only 1-2 nuclei, while multinuclear cells (≥ 3 nuclei) did not show distinctive TRAP-staining in every case. There were no statistical effects to be found between the different biomaterials in the evaluation of TRAP-positive cells (Fig. 6, Table 6).

SEM and histomorphometric analysis

To determine the influence of the calcium phosphate based biomaterials on the key function of human osteoclasts, namely bone resorption, PBMCs together with the triturated biomaterials were cultured on bovine bone slices for 21 d. The area fractions of resorbed bone (resorption pits) on the bone slices were then assessed by SEM, to measure the rate of

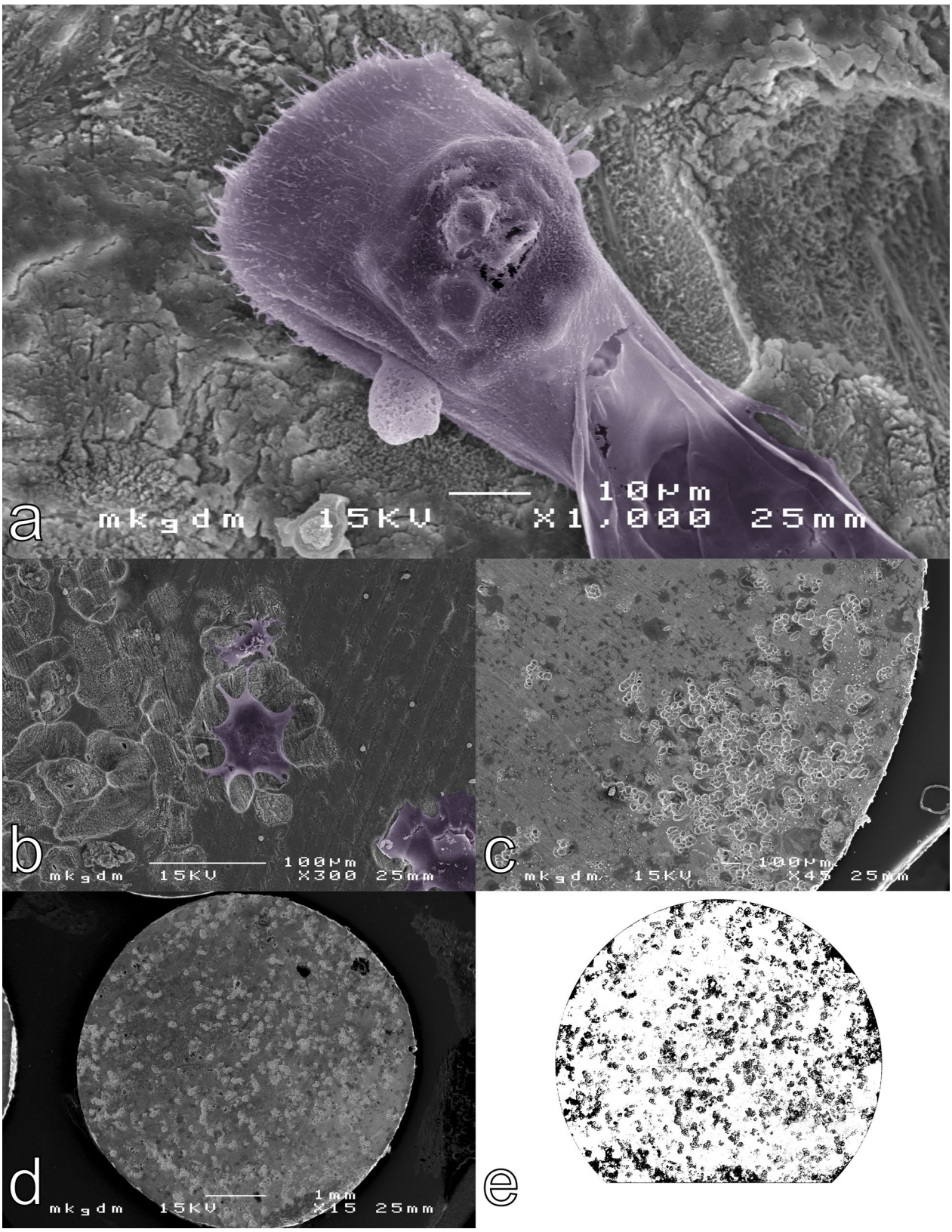

Fig 2. SEM. Detailed view of an active osteoclast (dyed purple) after phagocytosis of biomaterial (BM4-Cerasorb) embedded in resorption pits, featuring polarized cell morphology and filopodia (**a**, image taken before taping of the bone slice). Starfish-shaped osteoclasts (**b**, dyed purple) surrounded by resorption pits (**b**, left half) and unscathed surface of a bone slice (**b**, right half). Bovine bone slice featuring distinct resorption pits assessed after cell removal (taping) (**c**). Histomorphometric assessment of bone resorption by scanning of a taped bone slice (**d**) and subsequent image processing (**e**).

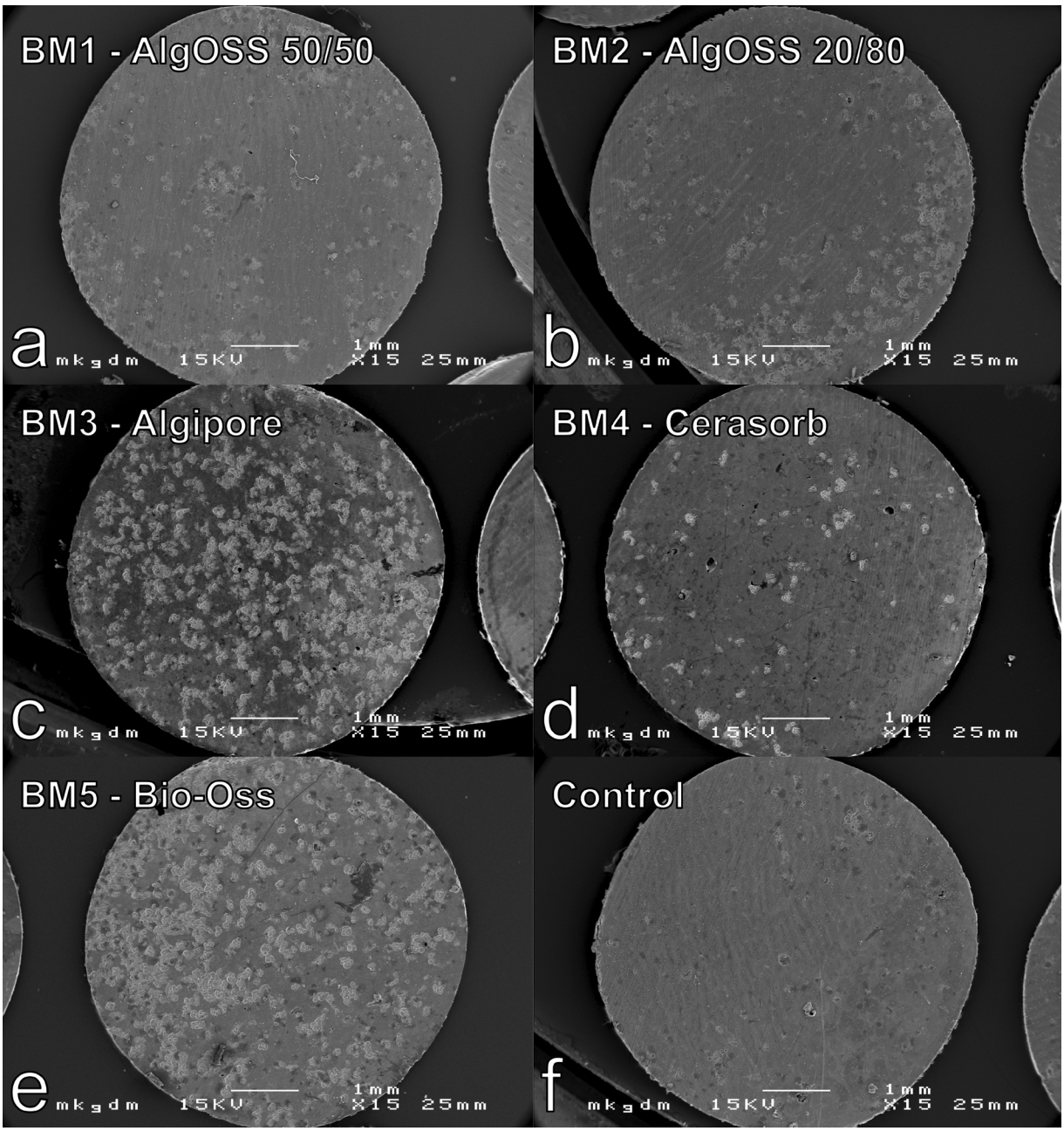

Fig 3. SEM overview of bone resorption assessed on bone slices. Fraction areas of resorbed bone reached from 5.56 ± 6.78 % (**f**, Control) to 9.82 ± 9.71 % (**c**, BM3 Algipore). BM5 (**e**, Bio-Oss) featured 7.86 ± 8.82 %. BM1 (**a**, AlgOSS 50/50) led to 6.96 ± 6.98 %, BM2 (**b**, AlgOSS 20/80) to 6.55 ± 7.09 % and BM4 (Cerasorb) to 6.68 ± 6.24 % of resorbed bone. Resorption pits appear as bright spots on the surface of the respective bone slices. (Images were taken after removal of cells and biomaterial particles.)

bone resorption. The average values of resorbed bone ranged from 5.56 ± 6.78 % (control group) to 9.82 ± 9.71 % BM3 (Algipore). BM5 (Bio-Oss) showed similar high rates of bone resorption (7.86 ± 8.82 %) to BM3. BM1 (AlgOSS 50/50) gave 6.96 ± 6.98 %, BM2 (AlgOSS 20/80) was 6.55 ± 7.09 % and BM4 (Cerasorb) resulted in 6.68 ± 6.24 % of resorbed bone (Fig. 3). A total of 110 bone slices were analyzed: 52 reached resorption values of 0-5 %, 26 reached 5-10 %, 28 reached 10-25 %, 2 reached > 25 % and 2 reached > 30 %.

It must be noted that the two purely hydroxyapatite-based biomaterials gave the highest rates of osteoclastic bone resorption (Fig. 3**c**,**e**). This was shown by regression analysis, which confirmed BM3 (Algipore, $p < 0.001$) and BM5 (Bio-OSS, $p = 0.029$) as significant predictive factors of more osteoclastic bone resorption (Fig. 7, Table 7).

In support of a sample size of five independent experiments (blood donors), *post-hoc* power analysis estimated an actual power of 99.9 % with a significance level of 5 % (alpha), a base rate of 3.5 % ($=e^{1.2498}$) bone resorption in the control group, and an effective bone resorption of 5 % ($=e^{1.6}$) in the biomaterial groups (BM1 to BM5).

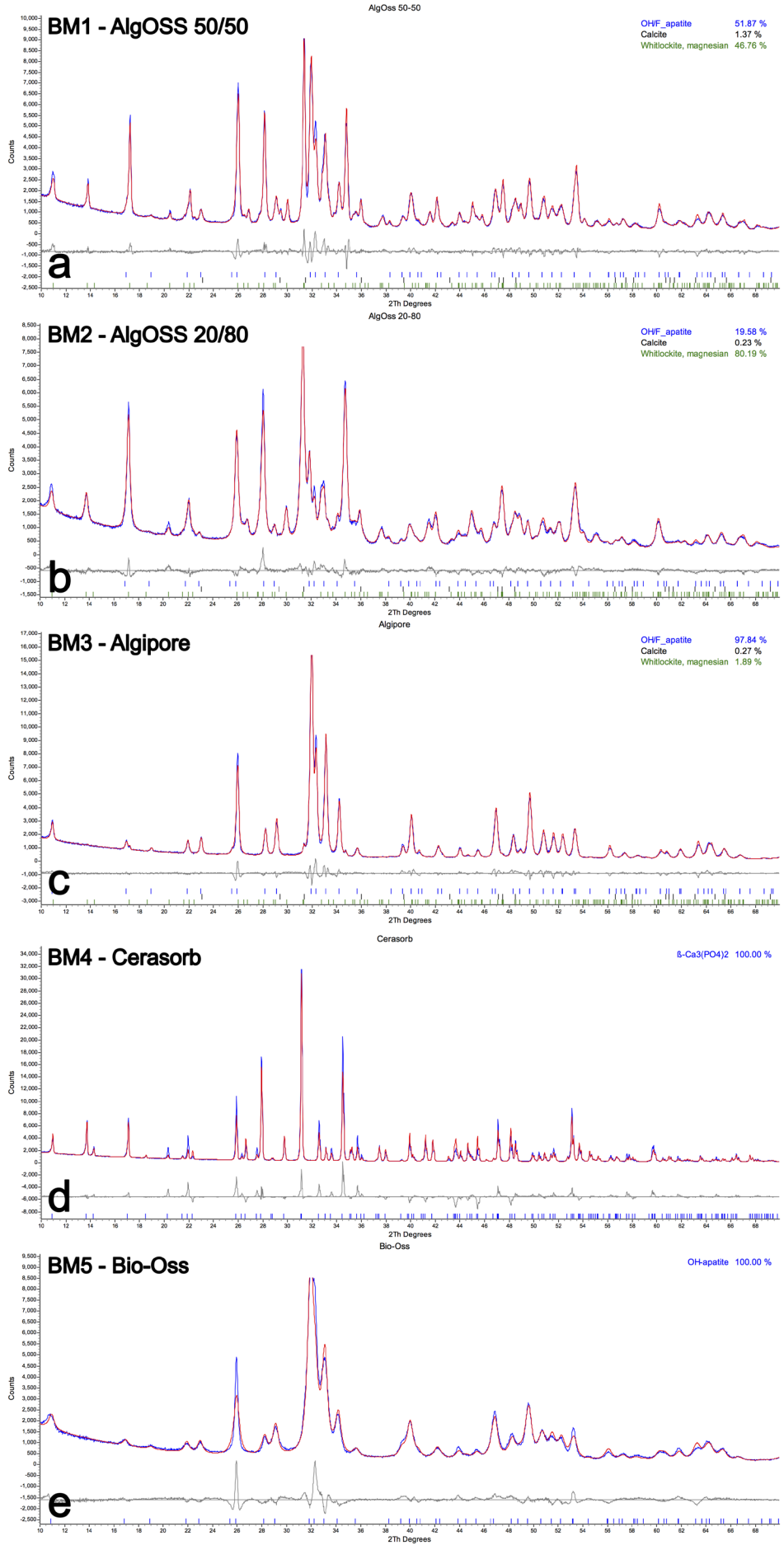

Fig 4. X-Ray diffraction analysis. Composition, crystallinity and crystallite sizes were estimated from X-ray diffraction powder patterns (CuK_{α} radiation) using the Rietveld method as implemented in the TOPAS program (version 4.1, Bruker AXS 2008).

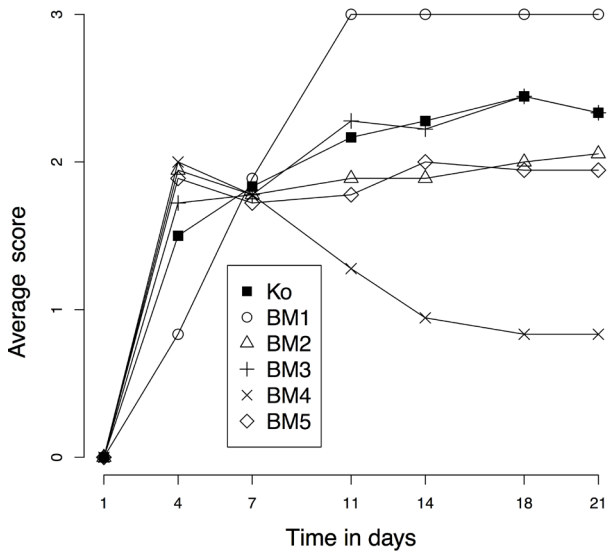

Fig 5. Descriptive analysis (run-sequence plot) of light microscopy. For statistical evaluation and results of light microscopy see Table 5.

Table 5. Light microscopy (generalized linear mixed model with Poisson distribution). The score of phenotypic cell morphology and number was estimated by intercept (*i.e.* control), time and biomaterial as dummy variables.

Factor	Estimate	Std. Error	*t* value	*p* (>|t|)
Intercept (= control)	1.76940	0.24086	7.346	< 0.001
Day	0.02586	0.01259	2.053	**0.049**
BM1 (AlgOSS 50/50)	0.36111	0.25780	1.401	0.172
BM2 (AlgOSS 20/80)	−0.16667	0.25780	−0.646	0.523
BM3 (Algipore)	0.03704	0.25780	0.144	0.887
BM4 (Cerasorb)	−0.81481	0.25780	−3.161	**0.004**
BM5 (Bio-Oss)	−0.21296	0.25780	−0.826	0.416

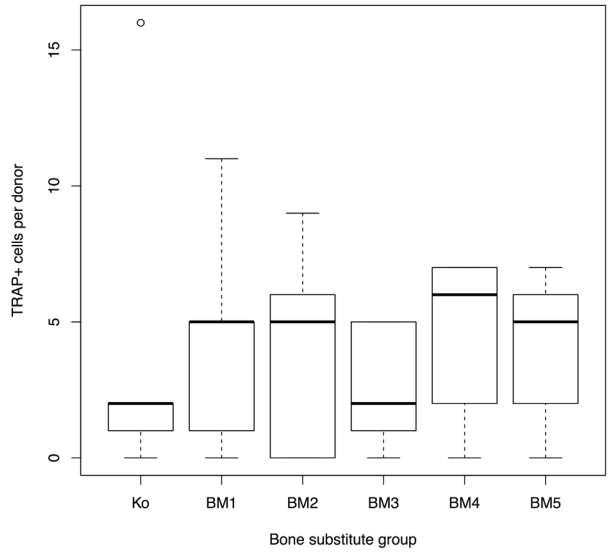

Fig 6. Descriptive analysis (boxplot) of TRAP-staining. The horizontal lines of the plot represent the smallest observation, lower quartile (Q1), median (Q2), upper quartile (Q3), and largest observation. A small circle indicates outliers. For statistical evaluation and results of TRAP-staining see Table 6.

Table 6. Evaluation of TRAP positive cells (generalized linear model with Poisson distribution). The cell count of TRAP positive cells was estimated by intercept (*i.e.* control) and biomaterial as dummy variables. (Since TRAP evaluation was done once at end of culture experiments, time was not applicable as a variable.)

Factor	Estimate	Std. Error	*z* value	*p* (>|z|)
Intercept (= control)	1.43508	0.21822	6.576	< 0.001
BM1 (AlgOSS 50/50)	0.04652	0.30508	0.152	0.879
BM2 (AlgOSS 20/80)	−0.04879	0.31244	−0.156	0.876
BM3 (Algipore)	−0.47957	0.35291	−1.359	0.174
BM4 (Cerasorb)	0.04652	0.30508	0.152	0.879
BM5 (Bio-Oss)	−0.04879	0.31244	−0.156	0.876

Discussion

This study focused on the *in vitro* bone resorption activity of human osteoclasts, under the influence of five different particulate bone substitute materials. For this purpose, peripheral blood mononuclear cells (PBMCs) were isolated and differentiated to osteoclasts by the addition of cytokines and cultured for 21 d. All the cultures were conducted according to a modified protocol of Flanagan and Massey (2003) for the differentiation of PBMCs. In order to assess effects on bone resorption, the PBMCs were not cultured directly on the respective biomaterials, but on bovine bone slices along with the small-sized biomaterial particles. To analyze time-dependent effects of the particulate bone substitute materials on the PBMCs, cell morphology and cell number were studied by light microscopy on glass cover slips during the cultivation. Cytochemical detection of osteoclast-like cells was performed by TRAP-staining at the end of the culture experiments. For the assessment of osteoclast mediated bone resorption, bone slices were studied by SEM, and the area fractions of resorbed bone determined by histomorphometry.

It was possible to differentiate PBMCs toward osteoclast-like morphology after the addition of RANKL, M-CSF, dexamethasone and vitamin D_3, in all cases. SEM of cells cultured on glass cover slips

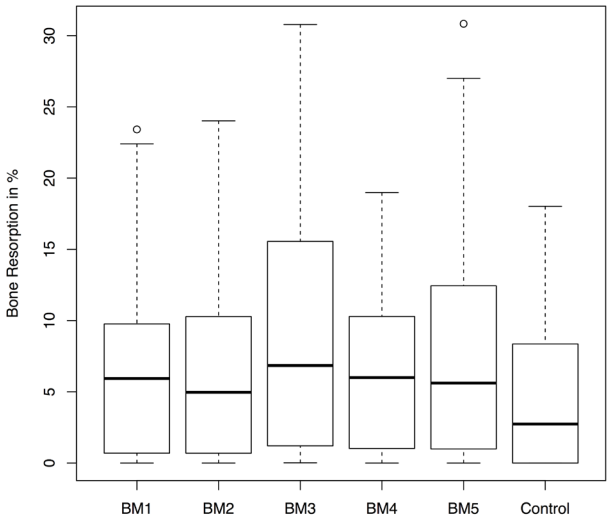

Fig 7. Descriptive analysis (boxplot) of SEM. The horizontal lines of the plot represent the smallest observation, lower quartile (Q1), median (Q2), upper quartile (Q3), and largest observation. A small circle indicates outliers. For statistical evaluation and results of SEM see Table 7.

Table 7. Histomorphometric analysis of bone resorption (generalized linear model with Poisson distribution). The area fractions of bone resorption were estimated by intercept (*i.e.* control) and the bone materials as dummy variables. (Since this evaluation was done once at the end of culture experiments, time was not applicable as a variable.)

Factor	Estimate	Std. Error	*z* value	*p* (>|z|)
Intercept (= control)	1.2498	0.2679	4.666	**< 0.001**
BM1 (AlgOSS 50/50)	0.2293	0.1626	1.410	0.158464
BM2 (AlgOSS 20/80)	0.1688	0.1640	1.030	0.303174
BM3 (Algipore)	0.5734	0.1560	3.675	**< 0.001**
BM4 (Cerasorb)	0.1880	0.1635	1.150	0.250345
BM5 (Bio-Oss)	0.3504	0.1600	2.189	**0.028584**

revealed multinuclear cells up to 300 μm in size. The evaluation of bone slices, in all groups, showed pronounced lacunar resorption and typical feeding traces of up to 400 μm in length. As the results of the cell culture experiments proved reproducible, this indicated that the modified Flanagan and Massey (2003) protocol was successful. Using PBMCs proved to be a useful method for generating human osteoclasts. Precursor cells were obtained rapidly. Venipuncture and differentiation, with the addition of RANKL and M-CSF, avoid the need for mesenchymal cell co-culture and consequently facilitate the evaluation of culture results (Friederichs *et al.*, 2015; Sabokbar and Athanasou, 2003). Nevertheless, the requirement for adding externally manufactured cytokines complicates the assessment of culture medium supernatants by standard assays (Lange *et al.*, 2009).

Differences between human and murine cells are well known, especially with regard to the effects of M-CSF and TGF-β. The use of human cells is preferable for *in vitro* studies involving the interaction of osteoclasts with biomaterials (Flanagan and Massey, 2003).

Unfortunately, the amount of PBMCs in peripheral blood is variable and depends on gender and age. Therefore, it is important to consider that the required volume of blood drawn can increase up to 40 mL per donor in order to reach the required total cell counts of about 5 x10^5 or more. A drawback of *in vitro* assays involving human osteoclasts, is that elaborate and difficult procedures are needed to ensure reproducible results (Sabokbar and Athanasou, 2003).

Understanding the phenotypic characteristics of osteoclast-like cells, as viewed by light microscopy (Kurihara *et al.*, 1990), makes it possible to analyze both multinuclearity and cell number per field of view in the context of studying the effect of electromagnetic fields on human osteoclasts cultures (Barnaba *et al.*, 2012). In addition, light microscopy based score systems are used in other areas, such as cartilage research or cytotoxicity assays (Changoor *et al.*, 2011; Grogan *et al.*, 2006). In order to determine the influence of the particulate biomaterials on the ability of PBMCs to develop osteoclast-like cell morphology during culturing, evaluations of cells cultured on glass cover slips, by light microscopy, were performed using a new scoring system. Analysis of PBMCs cultures revealed that all groups scored 0 on day 1 of culture, increased by day 4 and reached similar scores by day 7. After day 7, cell morphology progressed differently in the five treatment groups.

Schilling *et al.* (2004) are the first to report signs of osteoclastic differentiation from day 4, and the current work confirmed this. Similarly, Sabokbar and Athanasou (2003) describe the second week as being crucial to cultivation. BM1 (AlgOSS 50/50) increased until day 11 and featured the highest overall scores. This indicated that these cells differentiated most rapidly to osteoclast-like morphology. The control group and BM3 (Algipore) behaved similarly, but featured slower differentiation throughout and reached the highest levels by the end of culture period. BM2 (AlgOSS 20/80) and BM5 (Bio-Oss) showed comparable results, but less than the control group and BM3 (Algipore). To summarize, BM1, BM2, BM3 and BM5 showed distinct differentiation, but did not differ significantly from the control.

In contrast, cells from the BM4 (Cerasorb) group developed regularly over the first week of cultivation,

but then featured decreasing cell differentiation from day 7 on. Inhibition of cell differentiation was statistically significant. This indicated a negative impact of BM4 (Cerasorb) on cell differentiation under these conditions. Keller *et al.* (2012) report cultivating human osteoclasts on 10 different biomaterials, using dentin as the control group. In their investigations BM4 (Cerasorb) leads to increased cell adherence, progress of differentiation until day 14, larger numbers of TRAP-positive multinuclear cells on day 28, and positive effects on resorption. Detsch *et al*. (2008) analyze the effects of HA and TCP biomaterials on osteoclast-like cells derived from a human monocytic leukemia lineage. They suggest that a higher concentration of calcium in a TCP environment inhibits osteoclasts. However, the inhibitory effects of TCP detected did not exactly correspond to such published reports. Furthermore, it was not possible to confirm the effect of BM4 (Cerasorb), as determined by the light microscopy score, with a comparable reduction of bone resorption as detected by SEM. Estimation of inter-rater reliability (IRR) for the semi-quantitative evaluation by light microscopy revealed moderate agreement (Fleiss' Kappa of 0.495). This indicated that evaluation studies of bone resorption by SEM remained of higher validity than those conducted by light microscopy.

For the cytochemical proof of osteoclast presence and quantification, TRAP-staining of the cells on glass cover slips was conducted at the end of culture and after final light microscopic assessment of cell differentiation. This cytochemical staining is the only defining characteristic that permits a cell to be classified as an osteoclast (Sabokbar and Athanasou, 2003). Only very few cells were recognized as TRAP-positive (cells with reddish to brownish staining with ≥ 3 nuclei). Mixed model analysis could not describe the statistical data either. As a consequence, TRAP-staining did not lead to any conclusive results. TRAP-positive staining similarly varies from reddish, purple, yellow and brown color (Hoshino *et al.*, 2010; Jorgensen *et al.*, 2002; Li *et al.*, 2009b; Narducci *et al.*, 2010; Newa *et al.*, 2011; Paloneva *et al.*, 2003; Schilling *et al.*, 2004; Winkler *et al.*, 2010). This low TRAP count was in clear contrast to light microscopy results (many multinucleated cells) and the bone resorption assay that featured distinct lacunar resorption throughout all groups. Alternatively, the measurement of TRAP from the supernatants is possible, because Kirstein *et al*. (2006) report a correlation between TRAP secretion and bone resorption. Staining of vitronectin receptors (VNR) or calcitonin receptors (CTR) with monoclonal antibodies is an alternative to TRAP-staining, but seems to show reduced dependability (Flanagan and Massey, 2003; Miyamoto and Suda, 2003; Sabokbar and Athanasou, 2003; Schilling *et al.*, 2004).

In order to assess the influence of the calcium phosphate-based biomaterials on bone resorption of human osteoclasts, PBMCs together with the triturated biomaterials, were cultured on bovine bone slices for 21 d and resorption pits were analyzed by determining their area fraction. Osteoclasts are solely dedicated to the resorption of bone and hard tissue (Kylmaoja *et al.*, 2015). In contrast to this, foreign body giant cells (FBGCs) are not able to resorb bone (ten Harkel *et al.*, 2015). Despite many cellular similarities between these two cell types, FBGCs seem to be able to dissolve the superficial mineral fraction of bone but they are not capable of resorbing the organic matrix of bone and are consequently incompetent for osteoclastic bone resorption (ten Harkel *et al.*, 2015). Resorption pits and osteoclastic feeding traces connected to cells featuring osteoclast-like morphology were detected by SEM. In all cases, these cells were cultured on bovine bone slices. Due to the lack of any other cell type capable of bone resorption, we were convinced that we were able to culture functional (bone resorbing) human osteoclasts. The observation of osteoclast-derived bone resorption by SEM corresponded to published information (Kleinhans *et al.*, 2015; Sabokbar *et al.*, 2003; Sabokbar *et al.*, 1998).

The smallest area fractions of bone resorption were observed in the control group. They increased from BM2 (AlgOSS 20/80), BM4 (Cerasorb), BM1 (AlgOSS 50/50), and BM5 (Bio-Oss) to BM3 (Algipore). BM3 and BM5 showed the highest absolute area fractions of bone resorption and Poisson regression confirmed that these results were significant. Consequently, the two substitute materials composed of pure HA resulted in the highest impact on resorption activity.

The stoichiometry of the tested biomaterials also differed significantly, ranging from pure phase β-TCP (BM4) or HA (BM5), combined calcium deficient ion substituted HA, ion substituted β-TCP and traces of calcite (BM1, BM2 and BM3). In general, HA ($Ca_{10}(PO_4)_6(OH)_2$) offers little chemical solubility (at 25 °C, −log (Ks) = 116.8) and is resorbed on a cellular basis with a slow *in vivo* biodegradation rate (Bauer, 2007; Chow, 2009). Solubility of HA changes when it is calcium deficient (at 25 °C, −log (Ks) ≈ 85) or ion substituted (F^-, at 25 °C, −log (Ks) = 120) (Dorozhkin, 2011). β-TCP is chemically more soluble (at 25 °C, −log (Ks) = 28.9) than HA and offers a higher biodegradation rate (Chow, 2009; Horch *et al.*, 2006). Similar to HA, ion substitution leads to changes in solubility of β-TCP (Mg^{2+}, at 25 °C, −log (Ks) ≈ 33) (Li *et al.*, 2009a). These differences in biodegradation seem to influence volume stability of regenerated bone significantly in favor of HA (Jensen *et al.*, 2012; Russmueller *et al.*, 2015).

Despite stoichiometric phase composition, solubility, and β-TCP to HA ratio, it is important to note that bioreactivity can be strongly influenced by crystallinity, crystallite size and particle size (Gallinetti *et al.*, 2014; LeGeros *et al.*, 2003). Assessment of crystallinity showed that all tested biomaterials were highly crystalline, presenting values ranging from 70 % (BM1) to 100 % (BM4). As this study was inspired by observations of the influence of small-sized particles on osteoclast function (Hallab and Jacobs, 2009; Sabokbar *et al.*, 2003; Sabokbar *et al.*,

1998), all biomaterials were ground down from their commercially available grain size and featured d_{50}-values ranging from 3.73 µm to 6.68 µm before being applied to the cultures. Such small-sized particles can be phagocytized and may directly influence cellular activity (Noordin and Masri, 2012; Sabokbar *et al.*, 2003; Wang *et al.*, 1997a; Wang *et al.*, 1997b). Osteoclastic bone resorption was mostly activated by small-sized HA particles.

Whether and how osteoclasts are activated by biomaterial chemical properties, their specific surface features and similarity to bone structure still needs to be elucidated in detail: Lange *et al.* analyze the immunological effects of HA and TCP, and reveal a significantly lower induction of GM-CSF and RANKL in the presence of TCP particles (Lange *et al.*, 2009). Lange´s research group also shows that larger TCP particles, which cannot be phagocytosed can cause a higher inflammatory response when compared to smaller particles. Therefore, they ask whether the absence or inefficiency of phagocytosis due to TCP particle size, shape, or surface, can induce cytotoxic effects (Lange *et al.*, 2011).

A limitation of the current study was that the use of osteoclast differentiation media (GM-CSF and RANKL) for differentiation of FBGCs inhibited detailed insight into immunological effects. As a consequence, the results may not completely correspond to the ability of the biomaterials to stimulate osteoclast differentiation. We were not able to rule out that giant cells were forced into an osteoclastic lineage by addition of GM-CSF and RANKL to the cultures. To evaluate this in detail, an experimental setting without the external addition of these cytokines is needed (Lange *et al.*, 2009).

Detsch *et al.* show the solubility of HA and TCP in buffered sodium chloride solution, revealing that TCP has a significantly higher degradation than HA. According to this, a higher concentration of calcium in the surrounding of TCP, inhibits osteoclasts (Detsch *et al.*, 2008). In contrast to this, Taylor *et al.* (2002) report higher calcium concentrations near HA surfaces inhibiting osteoclast differentiation. Similar effects are described by Shiwaku *et al.* (2015).

Given that in the current study cell differentiation was conducted on bovine bone slices and particulate biomaterial particles were added once at the beginning of culture, the granules were able to sediment onto the bone slices and were not affected by changing the culture medium. Published work mostly reveals work done by direct cultivation of cells on plates or discs made out of biomaterial with dentin chips serving as control group. The possible comparison of our findings with those of others is limited, but a favorable role of HA can also be deduced (Keller *et al.*, 2012; Schilling *et al.*, 2004; Zhang *et al.*, 2012).

Keller *et al.* cultivated human osteoclasts on 10 different biomaterials and report that HA-based biomaterials (Tutogen bovin and Tutogen human) increase nuclei count and resorption, but they find no increase formation of mature osteoclasts (Keller *et al.*, 2012). Detsch *et al.* cultured osteoclast-like-cells deriving from a human monocytic leukemia cell line on HA and TCP ceramics. HA increases the formation of giant cells and significantly more and larger lacunae are detected. The count of TRAP-positive multinuclear cells is similar between the HA and TCP group (Detsch *et al.*, 2008). Taylor *et al.* reports the detection of fewer neonatal rabbit osteoclasts, less typical morphology, less frequent and smaller lacunae, and less resorption when cells are cultured on pure Bio-Oss plates after 4 d. Here, bovine cortical bone serves as a control (Taylor *et al.*, 2002). Similarly, Perotti *et al.* (2009) reports slower bone resorption of osteoclasts on Bio-Oss plates than on bovine bone. As these results are based on different study setups (processing of biomaterial, cultivation length and cell line used), in future, a standard assay for the evaluation of cell based resorption effects should be established to facilitate the comparison of these various reports (Kleinhans *et al.*, 2015). For example, Schilling *et al.* (2004) recommend the simultaneous use of dentin as a control, so as to allow comparison of biomaterials. The so-called resorbability coefficient (RRC) describes the ratio between resorption of biomaterial and resorption of dentin within the very same culture (Keller *et al.*, 2012; Schilling *et al.*, 2004). Co-culture systems are developed to gather information concerning bidirectional communication of osteoclasts and osteoblasts (Atkins *et al.*, 2005; Narducci *et al.*, 2010). However, there is currently no model for the simultaneous analysis of osteoconductive and osteoinductive features of bone substitutes (Keller *et al.*, 2012). As a consequence, a standardized and easy to conduct *in vitro* assay, such as the one presented here, may be a valuable supplement.

ten Harkel *et al.* (2015) claim that resorbable bone graft substitutes, such as calcium phosphates, should allow for remodeling by bone resorbing osteoclasts that is important for normal bone homeostasis, bone coupling, and osteogenesis. Culturing of PBMCs on bone slices and studying osteoclastic bone resorption may be valuable. At sites of bone augmentation and regeneration, osteoconductive ingrowth commonly starts at the border between endogenous bone and the biomaterial, resulting in a so-called bioactive area (Pearsall *et al.*, 1992; van Blitterswijk *et al.*, 1985). Any promotion or impairment of the osteoclast-osteoblast coupling may influence augmentation success (Kylmaoja *et al.*, 2015). The current study was designed based on observations of the role of this bioactive area between endogenous bone and biomaterial, and was inspired by observations of the influence of small-sized particles on osteoclast function (Sabokbar *et al.*, 2003; Sabokbar *et al.*, 1998; Wang *et al.*, 1997b). Consequently, it was shown that an addition of small-sized hydroxyapatite particles could improve the performance of conventional biomaterials. The next step would be to assess

whether these *in vitro* results correlate with the behavior of the studied bone substitute materials *in vivo* (Lange *et al.*, 2009; Zhang *et al.*, 2012).

Conclusions

The influence of different particulate bone substitute materials on human osteoclasts that were cultured from peripheral blood mononuclear cells *in vitro* was demonstrated. It was possible to show that small-sized particles of the purely hydroxyapatite-based biomaterials Algipore and Bio-Oss significantly enhance osteoclast-mediated bone resorption. As a limitation, assessment of differences in cell morphology, as observed by light microscopy, may have been influenced by the inaccuracy of this semi-quantitative method. Nevertheless, our results indicated that further study of the cellular effects of hydroxyapatite-based biomaterials could be revealing.

Acknowledgements

The authors want to thank AlgOss Biotechnologies for providing the biomaterials AlgOSS 50/50, AlgOSS 20/80 and Algipore. AlgOss Biotechnologies supported the author Else Spassova in the form of a salary, but did not have any additional role in the study design, data collection and analysis, decision to publish, or preparation of the manuscript. All other authors declare no conflict of interest.

References

Amini AR, Laurencin CT, Nukavarapu SP (2012) Bone tissue engineering: recent advances and challenges. Crit Rev Biomed Eng **40**: 363-408.

Atkins GJ, Kostakis P, Welldon KJ, Vincent C, Findlay DM, Zannettino AC (2005) Human trabecular bone-derived osteoblasts support human osteoclast formation *in vitro* in a defined, serum-free medium. J Cell Physiol **203**: 573-582.

Baldini N, De Sanctis M, Ferrari M (2011) Deproteinized bovine bone in periodontal and implant surgery. Dent Mater **27**: 61-70.

Barnaba SA, Ruzzini L, Di Martino A, Lanotte A, Sgambato A, Denaro V (2012) Clinical significance of different effects of static and pulsed electromagnetic fields on human osteoclast cultures. Rheumatol Int **32**: 1025-1031.

Bauer TW (2007) An overview of the histology of skeletal substitute materials. Arch Pathol Lab Med **131**: 217-224.

Changoor A, Tran-Khanh N, Methot S, Garon M, Hurtig MB, Shive MS, Buschmann MD (2011) A polarized light microscopy method for accurate and reliable grading of collagen organization in cartilage repair. Osteoarthritis Cartilage **19**: 126-135.

Chow LC (2009) Next generation calcium phosphate-based biomaterials. Dent Mater J **28**: 1-10.

Destainville A, Champion E, Bernache-Assollant D, Laborde E (2003) Synthesis, characterization and thermal behavior of apatitic tricalcium phosphate. Mater Chem Phys **80**: 269-277.

Detsch R, Boccaccini AR (2015) The role of osteoclasts in bone tissue engineering. J Tissue Eng Regen Med **9**: 1133-1149.

Detsch R, Mayr H, Ziegler G (2008) Formation of osteoclast-like cells on HA and TCP ceramics. Acta Biomater **4**: 139-148.

Dorozhkin SV (2011) Calcium orthophosphates: occurrence, properties, biomineralization, pathological calcification and biomimetic applications. Biomatter **1**: 121-164.

Flanagan AM, Massey HM (2003) Generating human osteoclasts *in vitro* from bone marrow and peripheral blood. Methods Mol Med **80**: 113-128.

Friederichs RJ, Brooks RA, Ueda M, Best SM (2015) *In vitro* osteoclast formation and resorption of silicon-substituted hydroxyapatite ceramics. J Biomed Mater Res A **103**: 3312-3322.

Gallinetti S, Canal C, Ginebra MP, Ferreira J (2014) Development and Characterization of Biphasic Hydroxyapatite/beta-TCP Cements. J Am Ceram Soc **97**: 1065-1073.

Grogan SP, Barbero A, Winkelmann V, Rieser F, Fitzsimmons JS, O'Driscoll S, Martin I, Mainil-Varlet P (2006) Visual histological grading system for the evaluation of *in vitro*-generated neocartilage. Tissue Eng **12**: 2141-2149.

Hallab NJ, Jacobs JJ (2009) Biologic effects of implant debris. Bull NYU Hosp Jt Dis **67**: 182-188.

Horch HH, Sader R, Pautke C, Neff A, Deppe H, Kolk A (2006) Synthetic, pure-phase beta-tricalcium phosphate ceramic granules (Cerasorb) for bone regeneration in the reconstructive surgery of the jaws. Int J Oral Maxillofac Surg **35**: 708-713.

Hoshino A, Iimura T, Ueha S, Hanada S, Maruoka Y, Mayahara M, Suzuki K, Imai T, Ito M, Manome Y, Yasuhara M, Kirino T, Yamaguchi A, Matsushima K, Yamamoto K (2010) Deficiency of chemokine receptor CCR1 causes osteopenia due to impaired functions of osteoclasts and osteoblasts. J Biol Chem **285**: 28826-28837.

Jensen SS, Broggini N, Hjorting-Hansen E, Schenk R, Buser D (2006) Bone healing and graft resorption of autograft, anorganic bovine bone and beta-tricalcium phosphate. A histologic and histomorphometric study in the mandibles of minipigs. Clin Oral Implants Res **17**: 237-243.

Jensen T, Schou S, Svendsen PA, Forman JL, Gundersen HJ, Terheyden H, Holmstrup P (2012) Volumetric changes of the graft after maxillary sinus floor augmentation with Bio-Oss and autogenous bone in different ratios: a radiographic study in minipigs. Clin Oral Implants Res **23**: 902-910.

Jorgensen NR, Henriksen Z, Sorensen OH, Eriksen EF, Civitelli R, Steinberg TH (2002) Intercellular calcium signaling occurs between human osteoblasts

and osteoclasts and requires activation of osteoclast P2X7 receptors. J Biol Chem **277**: 7574-7580.

Kao ST, Scott DD (2007) A review of bone substitutes. Oral Maxillofac Surg Clin North Am **19**: 513-521.

Keller J, Brink S, Busse B, Schilling AF, Schinke T, Amling M, Lange T (2012) Divergent resorbability and effects on osteoclast formation of commonly used bone substitutes in a human *in vitro*-assay. PLoS One **7**: e46757.

Kirstein B, Chambers TJ, Fuller K (2006) Secretion of tartrate-resistant acid phosphatase by osteoclasts correlates with resorptive behavior. J Cell Biochem **98**: 1085-1094.

Kleinhans C, Schmid FF, Schmid FV, Kluger PJ (2015) Comparison of osteoclastogenesis and resorption activity of human osteoclasts on tissue culture polystyrene and on natural extracellular bone matrix in 2D and 3D. J Biotechnol **205**: 101-110.

Kurihara N, Chenu C, Miller M, Civin C, Roodman GD (1990) Identification of committed mononuclear precursors for osteoclast-like cells formed in long term human marrow cultures. Endocrinology **126**: 2733-2741.

Kylmaoja E, Nakamura M, Tuukkanen J (2015) Osteoclasts and remodeling based bone formation. Curr Stem Cell Res Ther **11**: 626-633.

Lange T, Schilling AF, Peters F, Haag F, Morlock MM, Rueger JM, Amling M (2009) Proinflammatory and osteoclastogenic effects of beta-tricalciumphosphate and hydroxyapatite particles on human mononuclear cells *in vitro*. Biomaterials **30**: 5312-5318.

Lange T, Schilling AF, Peters F, Mujas J, Wicklein D, Amling M (2011) Size dependent induction of proinflammatory cytokines and cytotoxicity of particulate beta-tricalciumphosphate *in vitro*. Biomaterials **32**: 4067-4075.

Laurie SW, Kaban LB, Mulliken JB, Murray JE (1984) Donor-site morbidity after harvesting rib and iliac bone. Plast Reconstr Surg **73**: 933-938.

LeGeros RZ, Lin S, Rohanizadeh R, Mijares D, LeGeros JP (2003) Biphasic calcium phosphate bioceramics: preparation, properties and applications. J Mater Sci Mater Med **14**: 201-209.

Li X, Ito A, Sogo Y, Wang X, LeGeros RZ (2009a) Solubility of Mg-containing beta-tricalcium phosphate at 25 degrees C. Acta Biomater **5**: 508-517.

Li X, Jiang G, Wu D, Wang X, Zeng B (2009b) Construction of a recombinant eukaryotic expression plasmid containing human calcitonin gene and its expression in NIH3T3 cells. J Biomed Biotechnol **2009**: 241390.

Miyamoto T, Suda T (2003) Differentiation and function of osteoclasts. Keio J Med **52**: 1-7.

Narducci P, Bortul R, Bareggi R, Nicolin V (2010) Clathrin-dependent endocytosis of membrane-bound RANKL in differentiated osteoclasts. Eur J Histochem **54**: e6.

Newa M, Bhandari KH, Tang L, Kalvapalle R, Suresh M, Doschak MR (2011) Antibody-mediated "universal" osteoclast targeting platform using calcitonin as a model drug. Pharm Res **28**: 1131-1143.

Noordin S, Masri B (2012) Periprosthetic osteolysis: genetics, mechanisms and potential therapeutic interventions. Can J Surg **55**: 408-417.

Paloneva J, Mandelin J, Kiialainen A, Bohling T, Prudlo J, Hakola P, Haltia M, Konttinen YT, Peltonen L (2003) DAP12/TREM2 deficiency results in impaired osteoclast differentiation and osteoporotic features. J Exp Med **198**: 669-675.

Pearsall AD, Spears R, Chokshi M (1992) The ultrastructural architecture of the tissue/hard-tissue replacement interface. J Oral Maxillofac Surg **50**: 375-384; discussion 384-375.

Perrotti V, Nicholls BM, Horton MA, Piattelli A (2009) Human osteoclast formation and activity on a xenogenous bone mineral. J Biomed Mater Res A **90**: 238-246.

Riachi F, Naaman N, Tabarani C, Berberi A, Salameh Z (2014) Comparison of morbidity and complications of harvesting bone from the iliac crest and calvarium: a retrospective study. J Int Oral Health **6**: 32-35.

Russmueller G, Moser D, Spassova E, Plasenzotti R, Poeschl PW, Seemann R, Becker S, Pirklbauer K, Eder-Czembirek C, Czembirek C, Perisanidis C, Ewers R, Schopper C (2015) Tricalcium phosphate based biocomposites for mandibular bone regeneration – A histological study in sheep. J Craniomaxillofac Surg 43: 696-704.

Sabokbar A, Athanasou NS (2003) Generating human osteoclasts from peripheral blood. Methods Mol Med **80**: 101-111.

Sabokbar A, Pandey R, Athanasou NA (2003) The effect of particle size and electrical charge on macrophage-osteoclast differentiation and bone resorption. J Mater Sci Mater Med **14**: 731-738.

Sabokbar A, Pandey R, Quinn JM, Athanasou NA (1998) Osteoclastic differentiation by mononuclear phagocytes containing biomaterial particles. Arch Orthop Trauma Surg **117**: 136-140.

Schaaf H, Lendeckel S, Howaldt HP, Streckbein P (2010) Donor site morbidity after bone harvesting from the anterior iliac crest. Oral Surg Oral Med Oral Pathol Oral Radiol Endod **109**: 52-58.

Schilling AF, Brink S, Korbmacher H, Amling M, Rueger J (2006) Osteoclasts and Biomaterials. Eur J Trauma **32**: 107-113.

Schilling AF, Linhart W, Filke S, Gebauer M, Schinke T, Rueger JM, Amling M (2004) Resorbability of bone substitute biomaterials by human osteoclasts. Biomaterials **25**: 3963-3972.

Schopper C, Ziya-Ghazvini F, Goriwoda W, Moser D, Wanschitz F, Spassova E, Lagogiannis G, Auterith A, Ewers R (2005) HA/TCP compounding of a porous CaP biomaterial improves bone formation and scaffold degradation – a long-term histological study. J Biomed Mater Res B Appl Biomater **74**: 458-467.

Sheikh Z, Abdallah MN, Hanafi AA, Misbahuddin S, Rashid H, Glogauer M (2015) Mechanisms of *in vivo*

degradation and resorption of calcium phosphate based biomaterials. Materials **8**: 7913-7925.

Shiwaku Y, Neff L, Nagano K, Takeyama K, de Bruijn J, Dard M, Gori F, Baron R (2015) The crosstalk between osteoclasts and osteoblasts is dependent upon the composition and structure of biphasic calcium phosphates. PLoS One **10**: e0132903.

Spassova E (2007) Chemistry, ultrastructure and porosity of monophasic and biphasic bone forming materials derived from marine algae. Materialwissenschaft und Werkstofftechnik **38**: 1027-1034.

Taylor JC, Cuff SE, Leger JP, Morra A, Anderson GI (2002) *In vitro* osteoclast resorption of bone substitute biomaterials used for implant site augmentation: a pilot study. Int J Oral Maxillofac Implants **17**: 321-330.

Teitelbaum SL (2000) Bone resorption by osteoclasts. Science **289**: 1504-1508.

ten Harkel B, Schoenmaker T, Picavet DI, Davison NL, de Vries TJ, Everts V (2015) The foreign body giant cell cannot resorb bone, but dissolves hydroxyapatite like osteoclasts. PLoS One **10**: e0139564.

Vaananen HK, Laitala-Leinonen T (2008) Osteoclast lineage and function. Arch Biochem Biophys **473**: 132-138.

van Blitterswijk CA, Grote JJ, Kuypers W, Blok-van Hoek CJ, Daems WT (1985) Bioreactions at the tissue/hydroxyapatite interface. Biomaterials **6**: 243-251.

Wang W, Ferguson DJ, Quinn JM, Simpson AH, Athanasou NA (1997a) Biomaterial particle phagocytosis by bone-resorbing osteoclasts. J Bone Joint Surg Br **79**: 849-856.

Wang W, Ferguson DJ, Quinn JM, Simpson AH, Athanasou NA (1997b) Osteoclasts are capable of particle phagocytosis and bone resorption. J Pathol **182**: 92-98.

Winkler T, Hoenig E, Gildenhaar R, Berger G, Fritsch D, Janssen R, Morlock MM, Schilling AF (2010) Volumetric analysis of osteoclastic bioresorption of calcium phosphate ceramics with different solubilities. Acta Biomater **6**: 4127-4135.

Yamada S, Heymann D, Bouler JM, Daculsi G (1997) Osteoclastic resorption of calcium phosphate ceramics with different hydroxyapatite/beta-tricalcium phosphate ratios. Biomaterials **18**: 1037-1041.

Yasuda H, Shima N, Nakagawa N, Yamaguchi K, Kinosaki M, Mochizuki S, Tomoyasu A, Yano K, Goto M, Murakami A, Tsuda E, Morinaga T, Higashio K, Udagawa N, Takahashi N, Suda T (1998) Osteoclast differentiation factor is a ligand for osteoprotegerin/osteoclastogenesis-inhibitory factor and is identical to TRANCE/RANKL. Proc Natl Acad Sci U S A **95**: 3597-3602.

Zhang Z, Egana JT, Reckhenrich AK, Schenck TL, Lohmeyer JA, Schantz JT, Machens HG, Schilling AF (2012) Cell-based resorption assays for bone graft substitutes. Acta Biomater **8**: 13-19.

Discussion with reviewers

Stefan Tangl: How did you determine sample size?
Authors: The conduction of three independent experiments (samples) as triplets (three repetitions within one independent experiment) is common in cell culture experiments. We exceeded this number by two, thus, a total of five independent experiments (five donors). In addition, each independent experiment was conducted as quadruple in our investigation.

The generation of human osteoclasts from peripheral blood mononuclear cells (PBMCs) remains an ongoing field of research with few novel data published within the last three years. Thus, the number of publications to make an *a priori* sample-size calculation is still very limited in 2017.

Since data to make an *a priori* sample size calculation was not available, we based our experimental set-up as described above. We conducted a *post-hoc* power analysis in support of our sample size (number of independent experiments).

With a significance level of 5 % (alpha), a base rate of 3.5=% (==$e^{1.2498}$) bone area resorption in the control group, and an effective bone area resorption of 5= % (== $e^{1.6}$) in the tested groups (biomaterial 1 to 5), for the sample size of 5 an actual power of 99.9= % was estimated.

Stefan Tangl: What results did you expect? Explain.
Authors: Our study was inspired by observations of Sabokbar *et al*. (1998) on the promoting influence of small diameter particles on osteoclast function (Such effects may lead to aseptic loosening of joint implants in orthopedic surgery). This led us to believe that all the particulate bone substitute materials will enhance the activity of human osteoclasts cultivated from precursor cells *in vitro*. In order to assess such effects on bone resorption behavior and cell morphology, the PBMCs were not cultured directly on the respective biomaterials but on bovine bone slices or glass cover slips along with small diameter biomaterial particles.

As expected, all five biomaterials led to higher rates of bone resorption than the control (without biomaterial). The average values of resorbed bone ranged from 5.56 ± 6.78 % (control group) to 9.82 ± 9.71 % BM3 (Algipore). BM5 (Bio-Oss) featured similar high rates of bone resorption (7.86 ± 8.82 %) as BM3 in SEM evaluation. BM1 (AlgOSS 50/50) led to 6.96 ± 6.98 %, BM2 (AlgOSS 20/80) to 6.55 ± 7.09 % and BM4 (Cerasorb) to 6.68 ± 6.24 % of resorbed bone.

Editor's note: The Scientific Editor in charge of this paper was Chris Evans